# Grain Refinement of Magnesium Alloys

DAVID H. StJOHN, MA QIAN, MARK A. EASTON, PENG CAO, and ZOË HILDEBRAND

The literature on grain refinement of magnesium alloys is reviewed with regard to two broad groups of alloys: alloys that contain aluminum and alloys that do not contain aluminum. The alloys that are free of aluminum are generally very well refined by Zr master alloys. On the other hand, the understanding of grain refinement in aluminum bearing alloys is poor and in many cases confusing probably due to the interaction between impurity elements and aluminum in affecting the potency of nucleant particles. A grain refinement model that was developed for aluminum alloys is presented, which takes into account both alloy chemistry and nucleant particle potency. This model is applied to experimental data for a range of magnesium alloys. It is shown that by using this analytical approach, new information on the refinement of magnesium alloys is obtained as well as providing a method of characterizing the effectiveness of new refiners. The new information revealed by the model has identified new directions for further research. Future research needs to focus on gaining a better understanding of the detailed mechanisms by which refinement occurs and gathering data to improve our ability to predict grain refinement for particular combinations of alloy and impurity chemistry and nucleant particles.

## I. INTRODUCTION

ACHIEVEMENT of a fine grain size generally leads to improved mechanical properties and structural uniformity of most metals and alloys. Thus, a fine grain size in castings is important for the service performance of cast products and is also important for the final properties of semifabricated products, *e.g.*, extrusions that are produced from cast billet. High-pressure die castings (HPDCs) normally have a fine microstructure because of the extremely high solidification rates that are achieved and do not need the addition of a grain-refining agent. However, the solidification rate in sand castings, permanent mold castings, and direct chill billet castings is much slower and a uniform fine microstructure can generally only be achieved in these castings by use of a grain-refining additive prior to casting.

Depending upon whether they are alloyed with aluminum, magnesium alloys can be generally classified into two broad groups: aluminum free and aluminum bearing. Aluminum-free alloys mainly refer to those containing zirconium or grain refined by zirconium such as ZE41, ZK60, WE43, AM-SC1, and ML10. These are an important high value added class of alloys that are based on the exceptional grain-refining ability of zirconium when added to alloys that do not contain aluminum. Aluminum bearing alloys such as AM50, AM60, and AZ91 comprise the basis of the current magnesium business and have been predominantly used in HPDC applications. The exceptional grain-refining ability of zirconium does not occur in these alloys, as aluminum and zirconium can readily form stable intermetallic phases, which are unfortunately ineffective as nucleants for magnesium grains. Currently, a suitable grain refiner, *i.e.*, reliable and easy to apply, does not exist for this group of alloys. It has long been anticipated that such a grain refiner would allow alloys such as AZ91 and AZ31 to be used more extensively in non-HPDC applications, particularly for AZ31, as the demand for high-quality extrusion billet increases. This is because grain refinement can effectively reduce hot tearing susceptibility during direct chill billet casting, provide fine-grained billet with improved extrusion properties, and ensure a uniform fine-grained recrystallized microstructure in extruded product. Such a microstructure would lead to both optimum mechanical and cosmetic properties of extruded profiles. Moreover, a fine-grain-sized billet product would be suitable as a feedstock material for semisolid forming processes. Another attraction of grain refinement is that it results in improved creep resistance for alloys that contain a hard divorced eutectic phase, as has been demonstrated by the AM-SC1 alloy.[1] This is because in the fully grain-refined state, the hard divorced eutectic phase exists at triple points and along the grain boundaries to help lock the grain boundaries and reduce grain boundary sliding. Grain refinement also favors corrosion resistance as a result of improved structural uniformity including a more continuous intergranular phase.[2]

The technical importance of grain refinement has naturally spurred a renewed interest in grain-refining magnesium alloys due to increased applications in automobiles. In the following, a brief review of the grain refinement of magnesium alloys is presented, followed by a detailed discussion of a generalized theory of grain refinement, and the application of this theory to grain refinement of magnesium alloys. Finally, challenges in grain refinement of both aluminum-free and aluminum-bearing magnesium alloys are highlighted.

DAVID H. StJOHN, CEO, CRC for Cast Metals Manufacturing (CAST), is with the University of Queensland, Brisbane, QLD 4072, Australia. Contact e-mail: d.stjohn@cast.crc.org.au MA QIAN, Lecturer, is with the Brunel Centre for Advanced Solidification Technology, School of Engineering and Design, Brunel University, West London UB8 3PH, United Kingdom. MARK A. EASTON, Research Fellow, is with the School of Physics and Materials Engineering, Monash University, Clayton, VIC 3800, Australia. PENG CAO and ZOË HILDEBRAND, Postgraduate Students, are with Materials Engineering, School of Engineering, The University of Queensland, Brisbane.

This article is based on a presentation made in the symposium entitled "Phase Transformations and Deformation in Magnesium Alloys," which occurred during the Spring TMS meeting, March 14–17, 2004, in Charlotte, NC, under the auspices of ASM-MSCTS Phase Transformations Committee.

## II. GRAIN REFINEMENT OF MAGNESIUM ALLOYS: CURRENT UNDERSTANDING AND TECHNICAL STATUS

### A. *Grain Refinement of Mg-Al–Based Alloys*

Since the late 1930s, a number of approaches have been developed to obtain grain refinement in magnesium alloys that contain aluminum. These are briefly summarized as follows.

#### 1. *Superheating*

In foundry practice, the majority of metals and alloys should not be heated above their liquidus any higher than is necessary because elevated temperature promotes oxidation, gas absorption, and grain coarsening.[3] Aluminum-bearing magnesium alloys, however, are an exception in that they benefit from high-temperature treatment in terms of grain refinement. This high-temperature treatment is usually termed superheating and was first described in a British patent granted in 1931.[4] The process involves heating the melt to a temperature well above the liquidus of the alloy (often in the range 180 °C to 300 °C) for a short time, followed by rapid cooling to, and short holding at, the pouring temperature. The grain-refining effect of superheating is affected by a large number of factors. Sections a and b summarize some generally accepted characteristics of this approach.

a. *Effect of alloy composition*

(1) Aluminum is a key element for successful grain refinement by superheating. The superheating effect does not occur to a marked extent with any system other than Mg-Al.[5,6,7] Also, high aluminum content magnesium alloys (>8 pct Al) are more readily grain refined by superheating than low aluminum content alloys.[5,6]
(2) Grain refinement by superheating is significantly affected by Fe and Mn. In general, high-purity Mg-Al alloys with low Fe and Mn contents are less susceptible to superheating treatment than alloys with high Fe and Mn contents.[6,7,8] In other words, Mg-Al alloys exhibiting the superheating effect should contain some Fe or Mn.
(3) A small amount of silicon favors grain refinement by superheating. However, this effect disappears at a high iron content.[6] Both Be and Zr have been found to inhibit grain refinement of magnesium alloys by superheating.[5] Titanium is also considered to be an inhibiting element.[5]

b. *Effect of process variables*

There appears to be a specific temperature range for maximum grain-refining efficiency by superheating, *e.g.*, 850 °C to 900 °C for a Mg-9 pct Al-2 pct Zn alloy according to Tiner.[7] Once sufficient treatment time is given to attain a fine grain size, there is no further refining effect to be gained through increasing holding time at the superheat treatment temperature or repeating the process.[6] Successful superheating requires rapid cooling from the superheat treatment temperature to the pouring temperature and pouring promptly. The superheating effect generally disappears upon remelting.

One hypothesis proposed for this process is that Al-Fe or Al-Mn-Fe intermetallics of suitable habit precipitate from the melt on cooling and subsequently act as nucleation centers for magnesium grains.[5] This is supported by the observations that Mg-Al alloys exhibiting the superheating effect contain some Fe or Mn. Recent work by Cao *et al.*[9] confirms that Fe is a grain refiner for high-purity Mg-Al alloys (Fe $<$ 10 ppm; Mn $<$ 10 ppm) when added in the form of $FeCl_3$, due to the formation of Al- and Fe-rich intermetallic particles. In addition, Byun *et al.*[10] have recently shown that different types of AZ91 microstructure can be produced by taking advantage of the assumption that $Al_8(Mn,Fe)_5$ particles are effective nucleants for magnesium grains. The temperature-solubility theory[11] is another major hypothesis proposed for superheating. It was suggested that the particles present at normal melt temperatures are too large in size and too few in number to provide good grain refinement, but at higher melt temperatures, they will dissolve into the melt and then re-precipitate as a large number of fine nucleation sites on cooling. The third major hypothesis proposed is the nucleation of magnesium grains on $Al_4C_3$ particles,[5] based on the assumption that there is obvious uptake of carbon from steel crucible walls at the very high superheating treatment temperature. Other mechanisms proposed include nucleation on magnesium oxides, aluminum oxides, or similar nonmetallic inclusions that form during the superheating process.[6,7] It is likely that there is more than one mechanism functioning in superheating.

Owing to the requirement for rapid cooling from the treatment temperature to pouring temperature, grain refinement by superheating is less practical for a large pot of melt on a commercial scale. Other shortcomings include excessive consumption of time and fuel/electricity and shortened life of the alloying vessels.

#### 2. *Carbon inoculation*

Carbon inoculation is another major grain-refining approach developed to date for Mg-Al–based alloys. The key step of this process is the introduction of carbon into molten magnesium. Reported methods of introducing carbon include, but are not limited to, graphite, paraffin wax, lampblack, organic compounds such as hexachloroethane ($C_2Cl_6$) and hexachlorobenzene ($C_6Cl_6$), carbides ($Al_4C_3$, SiC, $CaC_2$), and bubbling the melt with carbonaceous gases (*e.g.*, CO, $CO_2$, $CH_4$).[5,6] Calcium carbide and hexachloroethane appear to work more satisfactorily than the other means, but the use of hexachloroethane causes environmental problems. The elements Be, Zr, Ti, and RE (rare earth elements) were found to interfere with this process.[5] The grain refinement achieved by carbon inoculation is in general comparable to that achieved by superheating.

Similar to superheating, carbon inoculation is effective only to magnesium alloys that contain aluminum.[11–14] In the literature, Mg-Al type alloys that can be effectively grain refined by carbon inoculation normally contain more than 2 pct Al. As such, there is a general consensus about the mechanism of carbon inoculation, *i.e.*, $Al_4C_3$ particles are effective nucleants for magnesium grains.[5,14] This is further supported by a recent development that the addition of an Al-$Al_4C_3$-SiC master alloy to AZ31 and AZ61 results in obvious grain refinement in both alloys,[15] where, following the $Al_4C_3$ hypothesis, the master alloy was reportedly made by reacting SiC with molten aluminum. Recent work by Yano *et al.*[16] shows that the nucleant particles found in the microstructure of an AZ91 alloy after carbon inoculation not only contain Al and C but also contain oxygen (O), suggesting that the nucleants are more likely to be a multi-

component compound containing Al, C, O, and even some other elements as well, rather than binary Al-C compounds.

Carbon inoculation is an effective approach for grain refinement of Mg-Al alloys. The major challenge is how to consistently introduce carbon into molten magnesium while on the other hand having no excess carbon left in the melt from a corrosion point of view.

3. *Grain Refinement by $FeCl_3$—the Elfinal Process*

The Elfinal process was invented by the metallurgists of I.G. Farbenindustrie (a pioneering German magnesium company) based on the hypothesis that iron particles could act as nucleation sites for magnesium grains. It was first reported in a Belgian patent granted in 1942,[17] which claimed that Mg-Al-Zn alloys (Al: 4 to 8.5 pct; Zn: 0.5 to 3 pct; no other elements were mentioned) could be grain refined by additions of 0.4 to 1.0 pct of anhydrous $FeCl_3$ at temperatures between 740 °C and 780 °C. Although the approach worked satisfactorily in terms of grain refinement, the mechanism proposed by its inventors failed to convince other metallurgists. Different mechanisms were subsequently proposed. According to Emley,[5] hydrolysis of $FeCl_3$ in the magnesium melt gives rise to copious hydrogen chloride (HCl) fumes, which then attack steel crucibles to liberate some carbon into the melt. The other mechanism proposed is that magnesium grains nucleate on Fe-Mn-Al particles that have a good crystallographic match with magnesium.[5] A recent detailed examination of this process has led to clarification of a number of issues:[9]

(1) The process leads to grain refinement when high-purity Mg-Al alloys are melted in carbon-free aluminum titanite crucibles, suggesting that refinement has little to do with the $Al_4C_3$ hypothesis proposed by Emley.[5]
(2) Al- and Fe-rich intermetallic particles rather than pure iron particles are observed in the central regions of many magnesium grains in both Mg-3 pct Al and Mg-9 pct Al alloys treated with different $FeCl_3$ additions, suggesting that magnesium grains nucleating on Fe-containing intermetallic particles of suitable habit give rise to grain refinement.
(3) Contrary to the observations made by Nelson,[6] iron can grain refine high-purity Mg-Al alloys containing little manganese ($<$10 ppm).

The Elfinal process has convincingly demonstrated that Fe is a grain refiner for Mg-Al alloys due most likely to the formation of Al- and Fe-rich intermetallic particles.[9] This has helped clarify many confusing phenomena observed in the grain refinement of Mg-Al alloys. Inhibiting elements also exist for this process such as Zr and Be (both elements are iron removal agents).[5] Although the Elfinal process leads to obvious grain refinement, Fe is notoriously detrimental to the corrosion resistance of magnesium alloys and, in addition, the release of Cl or HCl is of great concern. Thus, this approach is less attractive than others.

4. *Native grain refinement by control of impurity level*

That high-purity Mg-Al alloys have a native fine grain structure was first reported by Nelson.[6] Recent work by Tamura and co-workers[8,18] further confirmed Nelson's observations. The mechanisms of native grain refinement remain unclear. The high-purity Mg-9 pct Al alloys used by Tamura *et al*. were prepared using distilled pure magnesium (99.99 pct) and high-purity aluminum (99.99 pct), but still contained 20 ppm of carbon. As such, they attributed the observed native grain refinement to the $Al_4C_3$ or Al-C-O nucleants that existed in the melt. It is unclear whether native grain refinement of high-purity Mg-Al alloys is conditional upon the C and Al contents. The difficulty of clarifying the role of carbon lies in the difficulty of how to accurately determine a trace level of carbon in a magnesium alloy. It should be pointed out that this process contradicts the Elfinal process in terms of the role of Fe in the grain refinement of high-purity Mg-Al alloys.[9]

5. *Grain refinement by means of other additives*

Apart from the use of carbon or carbonaceous substances and $FeCl_3$, many other additives have been tried. These include Sr, RE, Th, Si, Ca, B, AlN, MgO, $TiB_2$, and TiC.[19,20,21] Of these additives, Sr was found to be effective only for pure magnesium or low aluminum content magnesium alloys (1 pct Al).[21] Other additives have reportedly led to grain refinement of Mg-Al alloys but none has yet been made available commercially. Boily and Blouin[19] have recently claimed that the use of microcrystalline $TiB_2$ and TiC particles (particle size: 0.5 to 30 $\mu$m) gives rise to grain refinement of Mg-Al alloys but no experimental details were disclosed.

In summary, a suitable grain refiner for Mg-Al alloys is still elusive and none of the approaches discussed has been satisfactory in a commercial sense. The two general directions of resolving the grain refinement problem of Mg-Al alloys are therefore either to find a new additive that will perform the task or to significantly improve the efficiency of an existing process. Either way requires a much better understanding of what controls the formation or poisoning of nucleant particles in a Mg-Al alloy.

## B. *Grain Refinement of Magnesium Alloys by Zr*

Zirconium is a potent grain refiner for magnesium alloys that contain little (impurity level) or no Al, Mn, Si, and Fe (zirconium forms stable compounds with these elements).[22] When added to these alloys, where the maximum solubility of Zr in molten pure magnesium at 654 °C is ~0.45 pct,[23] Zr can readily reduce the average grain size to about 50 $\mu$m from a few millimeters at normal cooling rates. Moreover, well-controlled grain refinement by Zr can lead to formation of nearly round or nodular grains,[24] which further enhance the structural uniformity of the final alloy. This exceptional grain-refining ability of Zr has led to the development of a number of commercially important magnesium alloys,[25] including a few recently developed sand casting creep-resistant alloys for automotive engine blocks.[1,26]

The most characteristic feature of the microstructure of a magnesium alloy containing more than a few tenths percent soluble zirconium is the Zr-rich cores that exist in most magnesium grains.[27] These Zr-rich cores are usually less than 15 $\mu$m in size at normal cooling rates. The cores are the result of peritectic solidification where Zr-rich magnesium solidifies first when magnesium is nucleated by the primary Zr particles. In the fully grain refined state, these Zr-rich cores generally appear with a nearly spherical or elliptical form and many contain a tiny particle in their central

regions.[27] Electron microprobe analyses of these particles showed that the majority were nearly pure Zr particles. On the other hand, little Zr was detected in most traversed areas that surrounded the cores, indicating that almost all Zr in solid solution is concentrated in the Zr-rich cores. The distribution of Zr in these cores was found to be inhomogeneous and to vary in a wide range, *e.g.*, from 0.5 to 3 pct. It has been found that many magnesium grains often contain more than one core, and they can exist anywhere inside a grain rather than just in the central region.[27,28]

Grain refinement of magnesium alloys by Zr is noticeable at low levels of soluble Zr.[22,29] Early work by Sauerwald[30] suggested that only the Zr that is dissolved in the liquid magnesium at the time of pouring is effective in causing grain refinement. Insoluble Zr such as undissolved Zr particles was believed to be irrelevant to grain refinement, despite both $\alpha$-zirconium and magnesium having the same type of crystal structure and nearly identical lattice parameters. This view appeared to be widely accepted until it was recently shown by Tamura *et al.*[31] that undissolved Zr particles actually play an important role in grain refinement. More recent work[32,33,34] has confirmed this observation and demonstrated that grain refinement of magnesium alloys by Zr is dictated by both soluble and insoluble Zr contents. Uptake of iron and settling of Zr particles are the two major factors affecting the soluble and insoluble Zr contents in a magnesium melt. Uptake of iron from a steel alloying vessel can quickly consume the soluble Zr content, particularly when the melt is held at a high temperature (>750 °C).[29] On the other hand, excess settling can lead to an obvious reduction in the number of active Zr particles in the melt. Either can cause an increase in the average grain size of the final alloy.[34,35] The soluble Zr content in a magnesium alloy is also affected by the alloy composition; *e.g.*, it has been found that the soluble Zr content is a function of the Zn content in Mg-Zn alloys and Zn and Zr form stable intermetallic compounds when the Zn content exceeds about 4 pct.[36]

A detailed examination of the size distribution of active zirconium particles that were observed at the centers of Zr-rich cores, in a fully grain-refined magnesium alloy, showed that the majority of particles were in the range between 1 and 5 $\mu$m in size when measured on polished sections, and that the most active group of particles were $\sim$2 $\mu$m when solidified in a mild steel cone mold.[37] A model has thus been developed for grain refinement of magnesium alloys by Zr from a microstructural point of view. This model relies upon nucleation on Zr particles in the size range between 1 and 5 $\mu$m (more favorably around 2 $\mu$m in size) and the formation of the maximum number of Zr-rich cores during solidification. Both of these conditions require that the melt contain the maximum soluble Zr content and a sufficient number of suitably sized undissolved Zr particles prior to pouring.

In general, grain refinement of aluminum-free magnesium alloys is well established both scientifically and commercially compared to the grain refinement of aluminum-bearing alloys. However, Zr is an expensive grain refiner and there appears to be no alternative to it. Reducing the consumption of zirconium grain refiner, and hence the cost of grain refinement, is therefore the major challenge that needs to be addressed. Understanding the detailed refinement mechanisms by which Zr works is essential for this purpose.

## III. A THEORY OF GRAIN REFINEMENT: THE ROLE OF SOLUTE AND PARTICLE POTENCY

Due to the importance of grain refinement to a broad range of aluminum alloys, considerable work has been carried out for over half a century to determine the mechanisms by which grain refinement occurs.[38–42] It is now generally accepted that both the potency of the nucleant particles (defined here as the undercooling required for nucleation, $\Delta T_n$) and the segregating power of the solute (defined as the growth restriction factor, $Q$) are critical in determining the final grain size.[43–46]

Easton and StJohn[45] developed a model that takes into account both $\Delta T_n$ and $Q$, and good agreement was found between this model and experimental results. The model was derived by assuming that in most melts constitutional undercooling is the dominant undercooling available once the thermal undercooling generated by the mold walls on pouring has quickly dissipated. The amount of thermal undercooling is dependent on cooling rate. Crystals nucleated on or near the mold walls due to the thermal undercooling can be swept into the bulk of the melt and, depending on their survival rate, contribute to the final grain size. This aspect is discussed elsewhere[47] and is not considered further in this article.

To simplify the model, it is also assumed that the actual temperature gradient in the melt is negligible or very low. This is reasonable due to the high thermal conductivity of the melt. Thus, the constitutional undercooling

$$\Delta T_c = m_l c_0 \left( 1 - \frac{1}{(1 - f_s)^p} \right) \qquad [1]$$

where $m_l$ is the slope of the liquidus line, $c_0$ is the composition of the alloy, $f_s$ is the solid fraction solidified, and $p = 1 - k$, where $k$ is the partition coefficient.

By taking the first derivative of Eq. [1] at $f_s = 0$, we find that the initial rate of development of constitutional undercooling is equal to the growth restriction factor $Q$. That is,

$$\frac{d\Delta T_c}{df_s} = m_l c_0 (k - 1) = \text{the growth restriction factor, } Q \qquad [2]$$

This relationship is true for either equilibrium or nonequilibrium Scheilian solidification.[41]

Further, if it is assumed that a nucleation event occurs when $\Delta T_c$ reaches $\Delta T_n$, then $f_s$ must correspond to the grain size as $f_s$ represents the amount of grain growth that occurs before it is interrupted by the next nucleation event. This assumption also assumes that potent nucleant particles are present at the point where $\Delta T_n$ is achieved. Due to the shallow temperature gradient present in the melt, a wave of nucleation events occurs from the mold walls toward the thermal center of the casting. Each new nucleation event occurs when growth of the previously nucleated grain generates constitutional undercooling equal to $\Delta T_n$. By rearranging Eq. [1], we can calculate the relative change in grain size with solute composition and particle potency where relative grain size (RGS) is

$$\text{RGS} = f_{s,n} = 1 - \left( \frac{m_l c_0}{m_l c_0 - \Delta T_n} \right)^{\frac{1}{p}} \qquad [3]$$

where $f_{s,n}$ is the amount of growth required to develop the undercooling, $\Delta T_n$, necessary for nucleation to occur.

Equation [3] can be used to show (Figure 1) the relationship between grain size and the combined effects of particle potency, $\Delta T_n$, and solute content of the alloys. Figure 1 shows that particle potency has a significant effect on grain size for all solute contents while solute content has a dramatic effect on grain size at low solute contents and very little effect at high solute contents.

The model can be simplified by assuming that the constitutional effects on the grain size are related to the initial rate of development of constitutional undercooling according to Eq. [2]. This assumption is particularly useful when potent nucleant particles are present. In this case, the grain size becomes related to $1/Q$.[45] Table I presents the data for calculating $Q$ for a range of elements when alloyed to magnesium. It can be seen that one of the reasons why Zr is an excellent refiner is that it generates very high values of $Q$ when small amounts are present in the magnesium as solute.

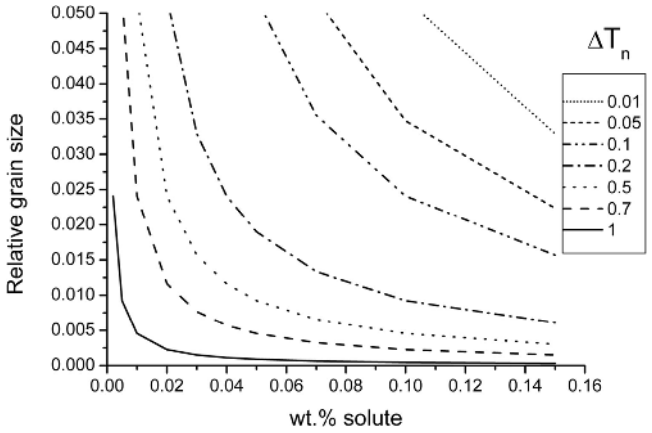


Fig. 1—Relative grain size *vs* solute content for a range of nucleant particle potencies, $\Delta T_n$, as calculated by Eq. [3]. The solute used is Ti added to pure Al.[51]

**Table I. Slope of the Liquidus Line, *m*, Equilibrium Distribution Coefficient, *k*, and Growth Restriction Factor, $m(k-1)$, of Various Alloying Elements in Magnesium***

| Element | $m$ | $k$ | $m(k-1)$ | System |
|---|---|---|---|---|
| Fe | −55.56 | 0.054 | 52.56 | eutectic |
| Zr | 6.90 | 6.55 | 38.29 | peritectic |
| Ca | −12.67 | 0.06 | 11.94 | eutectic |
| Si | −9.25 | ≈0.00 | 9.25 | eutectic |
| Ni | −6.13 | ≈0.00 | 6.13 | eutectic |
| Zn | −6.04 | 0.12 | 5.31 | eutectic |
| Cu | −5.37 | 0.02 | 5.28 | eutectic |
| Ge | −4.41 | ≈0.00 | 4.41 | eutectic |
| Al | −6.87 | 0.37 | 4.32 | eutectic |
| Sr | −3.53 | 0.006 | 3.51 | eutectic |
| Ce | −2.86 | 0.04 | 2.74 | eutectic |
| Sc | 4.02 | 1.65 | 2.61 | peritectic |
| Yb | −3.07 | 0.17 | 2.53 | eutectic |
| Y | −3.40 | 0.50 | 1.70 | eutectic |
| Sn | −2.41 | 0.39 | 1.47 | eutectic |
| Pb | −2.75 | 0.62 | 1.03 | eutectic |
| Sb | −0.53 | ≈0.00 | 0.53 | eutectic |
| Mn | 1.49 | 1.10 | 0.15 | peritectic |

*The value of $Q$ is calculated by $C_o m(k-1)$, where $C_o$ is the composition of the alloy. Note that experimental data was not available for some of the binary systems, in which case theoretical calculation values were used.[21]

Replotting the data in Figure 1 against $1/Q$ gives a series of straight lines. Figure 2 represents a typical grain size, $d$, *vs* $1/Q$ plot showing the relationship

$$d = a + b/Q \qquad [4]$$

It has recently been shown[48] that the slope, $b$, is related to the potency of the nucleant particles where a steeper slope corresponds to a lower potency, and the intercept, $a$, corresponds to the number of particles that actually nucleate grains at infinite values of $Q$. Theoretically, $a$ can decrease to zero for an infinite number of particles, as shown in Figure 2(b). However, the minimum achievable grain size for an alloy defined by a particular value of $Q$ is given by the point at $Q$ on the line of slope $b$ that passes through the origin (*i.e.*, for an infinite number of particles). Also, $a$ decreases according to a cube root relationship as the amount of grain refiner added is increased.[48] Thus, Eq. [4] becomes

$$d = \frac{a'}{\sqrt[3]{\rho f}} + \frac{b'\Delta T_n}{Q} \qquad [5]$$

where $\rho$ is the density of nucleant particles and $f$ is the fraction of these particles that are activated.

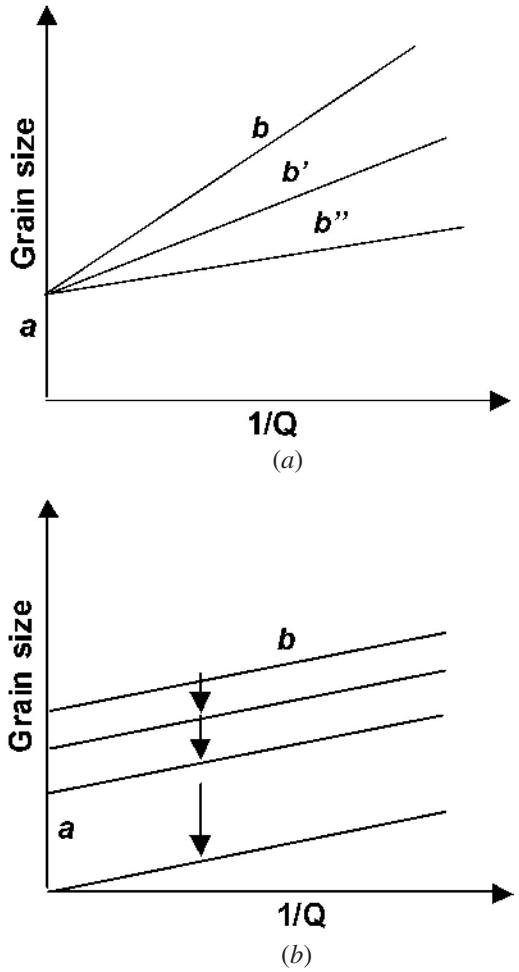


Fig. 2—(*a*) Effect of changing the nucleant particle potency on the gradient $b$ while keeping the number of particles constant. Particles that produce a slope $b''$ are the most potent particles. (*b*) Effect of adding more particles on the value of $a$, while keeping the potency constant.

These relationships have been verified by a large number of experiments on a broad range of aluminum alloys.[48]

The application of the theory to magnesium alloys is more difficult than to aluminum alloys. In aluminum alloys, we can quantify the amount and relative potency of particles relatively easily. This is not easy to do in magnesium alloys. For example, when Zr is added, the Zr particles dissolve to different extents depending on the initial particle size and processing conditions. The situation is even more difficult for Mg-Al–based alloys because, in most cases, we do not clearly know what the nucleant particles are, let alone how to predict their potency and number. However, the theory can be used to gain insight into the factors that affect the grain-refining capacity of a range of magnesium alloys.

## IV. GRAIN REFINEMENT OF MAGNESIUM ALLOYS: EXPERIMENTAL OBSERVATIONS AND DISCUSSION

Figure 3 shows the grain size resulting from binary additions of Zr, Al, Zn, Ca, and Si plotted against $Q$, as presented by Lee *et al*.[21] Viewing the data in this traditional way does not provide as much information as a plot of grain size versus $1/Q$, as shown in Figure 4. By replotting grain size against $1/Q$, we can separate the effect of alloy composition and focus on the factors related to the potency and relative number of the particles responsible for nucleating grains. However, in the case of the alloys studied here, it needs to be realized that the nucleant particle additions are not controlled and this will affect interpretation of the data. The main problem is that the elemental additions may have added known or unknown nucleant particles. In the case of the Mg-Zr system, Zr particles are added but the exact number is not known due to different degrees of dissolution of Zr particles into the magnesium melt. However, for the other elemental additions, it will be assumed that the elemental additions may change the chemistry or structure of the impurity particles that act as the nucleating substrates but not their number. This assumption appears to be reasonable as the intercepts, $a$, are approximately similar. If large numbers of nucleant particles are added with each increment of elemental addition, then the intercept will decrease substantially as in the case when Zr is added. It should also be noted that the gradient $b$ will only increase if nucleant particles are added with each increment of elemental addition and therefore the gradient will underestimate the potency of the nucleant particles. Despite the need to consider this aspect, analysis of the data presented in Figure 4 reveals important information.

By analyzing Figure 4, it can be more clearly seen that the values of the slope $b$ and the intercept $a$ vary considerably, as shown in Table II. The very high value of $b$ (Table II) for the Mg-Al alloys shows that there are nucleant particles of very low potency present. Aluminum forms intermetallics with many impurity elements, particularly Fe.[5,6,8,9] Some of these intermetallics have good potency while others have very low potency. The likelihood of low potency nucleant particles being present appears to be affected by the purity of the base magnesium used to make the alloy with higher purity providing a smaller grain size.[6,21] Contradicting these observations is the fact that Fe can refine magnesium alloys.[9] Thus, the relationship between purity and potency is complicated and at present is not well understood. This complexity probably explains why a suitable reliable grain refiner for Mg-Al–based alloys remains elusive.

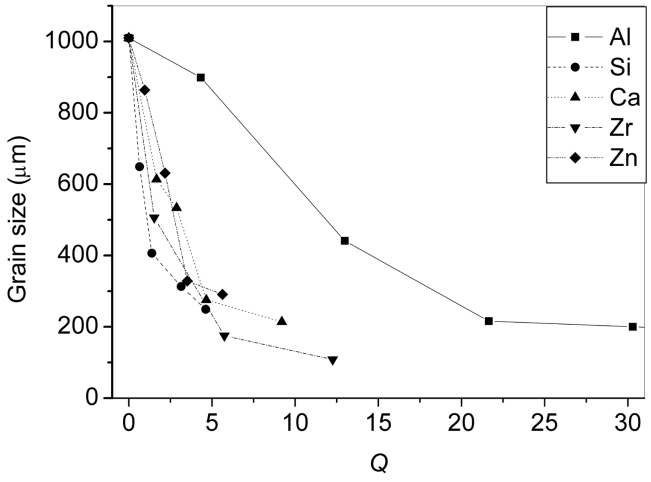


Fig. 3—The grain size of binary magnesium alloys with Al, Zr, Zn, Ca, and Si plotted against the growth restriction factor $Q$. The data are taken from Lee *et al*.[21]

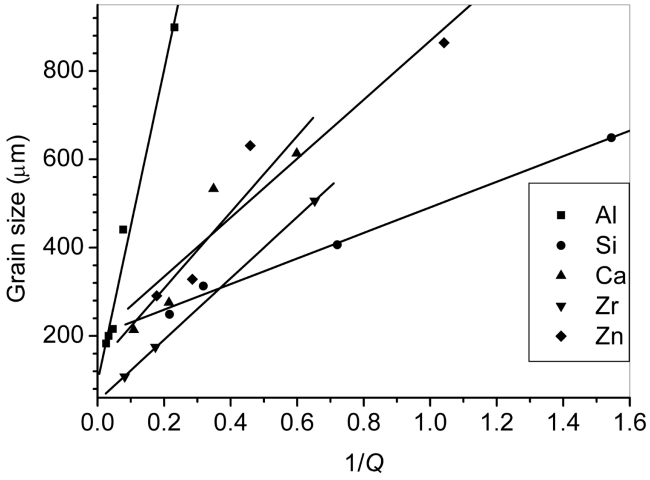


Fig. 4—The grain size of binary magnesium alloys with Al, Zr, Zn, Ca, and Si plotted against the growth restriction factor $1/Q$.

**Table II. Values of the Gradient $b$ and Intercept $a$ of Grain Size *vs* $1/Q$ Lines for Mg Binary Alloys with Al, Ca, Zr, Si, and Zn Presented in Figure 4***

| Element | Gradient $b$ ($\mu$m K) | Intercept $a$ ($\mu$m) | $R^2$ |
|---|---|---|---|
| Al | 3534 | 95.9 | 0.98 |
| Ca | 864 | 135 | 0.88 |
| Zr | 695 | 52.5 | 1.0 |
| Si | 290 | 202 | 0.99 |
| Zn | 668 | 201 | 0.90 |

*$R^2$ is the correlation coefficient. The data are obtained by assuming the total measured concentration of the binary element is present as solute. This assumption is probably correct for all elements except Zr; although the total Zr contents are below the solubility limit, Zr particles remain undissolved in the melt.

From Figure 4, it appears that Zn and Ca behave in a similar manner and may contain nucleant particles of the same type as the *b* values are similar, although the particles in the Mg-Zn alloy may be slightly more potent (Table II). The potency of these unknown particles (which may or may not contain Zn or Ca) as nucleating substrates is much higher than those in the Mg-Al system analyzed in this work (*b* values of 700 to 900 compared to 3500, Table II).

The most surprising result arising from Figure 4 is the very low value of *b* for the Mg-Si binary alloys. This implies that the nucleant particles present in this alloy are very potent. It is known that SiC can be a nucleant for magnesium,[49] and it is possible that SiC is formed if carbon is present as an impurity element. Despite the very good potency, the value of the intercept *a* is comparatively high, implying that there are fewer particles present in the melt compared with the other binary alloys.

The *b* value for Zr is similar to the Mg-Zn alloy, but this does not imply similar potency as the Zr results include the deliberate addition of Zr particles. Thus, the plot for Zr is steeper in Figure 4 than it should be because the value of *Q* is overestimated due to some of the Zr remaining as solid particles rather than as solute Zr and due to increasing numbers of Zr particles with each increase in Zr content. Figure 5 is a schematic showing how the data are skewed and that the actual value of *b* is in fact a much lower value. The data plotted in Figure 4 assume that the total Zr added to the melt was dissolved. However, this is not correct as some Zr particles remain undissolved in the melt. Therefore, the *Q* value of each plotted point needs to be corrected, as shown in Figure 5, by moving horizontally to the right to reflect a lower *Q* value than that calculated using the total Zr content (*e.g.*, point C shifts to point C′). Also, in order to calculate the correct *b* value (or potency) for Zr particles, the number of particles needs to remain constant. However, each further addition of Zr means that more Zr particles remain undissolved in the melt. To correct for the increasing number of Zr particles, points A and B need to not only move horizontally to the right to correct for a lower *Q* value, but must also move vertically upward to A′ and B′ to reduce the number of particles to equal the number present in alloy C as this reduction would lead to a larger grain size. A line drawn through A′, B′, and C′ in Figure 5 then defines the correct *b* value for Zr particles. However, it is difficult to quantify the different contributions of the Zr particles and the Zr solute. The additions made were all below the peritectic composition of 0.45 pct Zr, which suggests that all the Zr particles should have dissolved. However, previous studies indicate that up to 50 pct of the Zr particles remain in the melt even at long holding times.[34,36,50] If the contribution of increasing numbers of Zr particles is removed, then *b* would have a much lower value as would be expected given the excellent crystallographic match between Mg and Zr. To obtain data with a constant number of Zr particles while changing the value of *Q* is very difficult and requires well-controlled experiments. Further work is in progress to generate the data required to improve the quantification of *b* and *a* for Mg-Zr alloy systems.

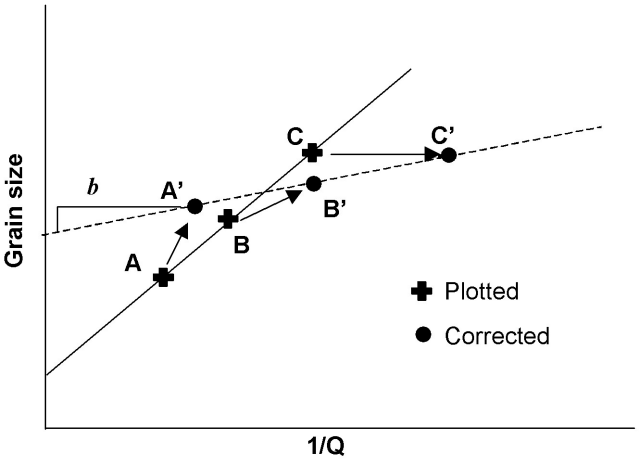


Fig. 5—A schematic plot showing that the plotted data presented in Fig. 4 for the Mg-Zr system are skewed compared to the data after correction for undissolved Zr and the increased number of Zr particles after each further addition of Zr.

It is clear that the information provided by Figure 4 allows conclusions to be drawn about the nature of the nucleant particles in terms of their potency and relative number, which can characterize the performance of new nucleant particles and identify whether the nucleant potency or number is more important in optimizing the grain refinement system. This model provides another analytical approach that can be used to identify potential grain-refining systems and information to complement, or in some cases without the need of, information gained from compositional analysis or crystallography of the particles. Through analysis of grain size *vs* 1/*Q* plots, opportunities for the design of new grain refiners may become apparent.

Due to the complicated role of impurities and the interaction of alloying elements, the data presented here cannot be used to draw conclusions about what may occur in associated ternary alloys or when using a different source of base alloying additions. It is likely that if this work were to be repeated using a number of different source materials, a range of *b* and *a* values would be obtained depending on whether the level of purity changes the composition and thus the crystallography of the nucleant particles (and thus *b*) or reduces the number of potent particles that nucleate the grains (and thus *a*). For example, Al forms intermetallics with most elements present or added to the melt leading to a large array of possible intermetallics that could be formed within different alloys. Also, the formation of the potent nucleants in the Mg-Si system of this study may not be formed in a carbon-free melt or when alloyed with aluminum as the conditions for the formation of SiC may not be present.

More data are needed to be able to use this model to identify the detailed mechanisms affecting grain refinement. By carrying out systematic work on superheating, native grain refinement and carbon inoculation for a range of alloys along a spectrum of *Q* values should reveal information that will improve our understanding of the mechanisms operating in these grain refinement methods. This understanding will then help us to define process and chemistry factors that will consistently achieve a fine grain size in Mg-Al–based alloys.

The model can also be applied to Zr additions to qualitatively show the effect of stirring, settling, and Zr loss on grain size. Figure 6 is a schematic representing the changes in grain size that can occur on the addition of Zr to an alloy designated as A. Alloy A sits on a line of slope *b′* as the nucleants naturally present in the unrefined alloy have poor potency and the intercept *a* is a large value because there are few particles that activate the nucleation of grains. The change from A to B occurs when Zr master alloy is dropped into the

melt but before stirring is applied. The grain size decreases due to the release of a few Zr particles, but $Q$ does not change significantly as little dissolution of Zr has occurred. However, alloy B sits on a line of slope $b''$ due to the addition of more potent particles. When stirring is applied, the Zr particles are distributed throughout the melt causing the grain size to decrease further to point C. In addition, stirring enhances the dissolution of Zr dramatically causing $Q$ to increase and the grain size to decrease along C to D. It is likely that these last two effects occur simultaneously with the grain size following a line between B and D. If further Zr master alloy is added, then the grain size will follow the line between D and E as the extra grain refiner will add both dissolved Zr and Zr particles. Further addition from E to F brings the soluble Zr to the maximum solubility limit according to phase equilibria. Further additions of master alloy beyond F will decrease the grains size but $Q$ will not increase further.

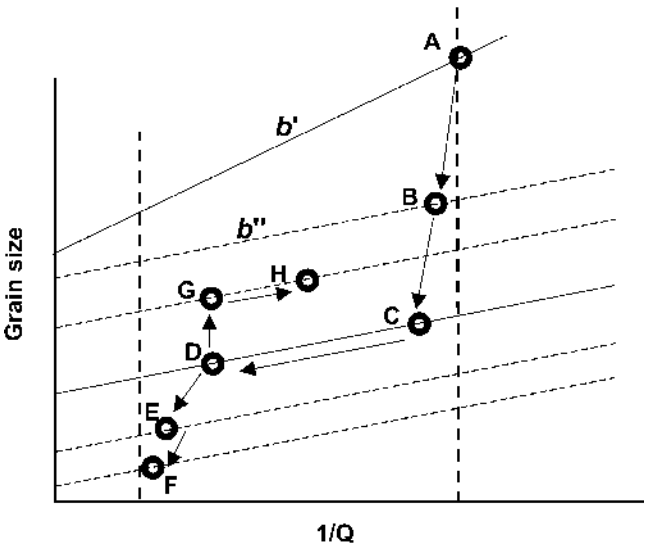


Fig. 6—A schematic representation of the changes in grain size during the addition of Zr master alloy to a Mg-0.5 pct Zn alloy as a function of the value of $1/Q$, the potency of nucleant particles, $b$, and the number of active nucleant particles. An elaboration of this model is provided in the text.

If a stirred melt of composition D is left to sit, then settling of Zr particles will occur, increasing the grain size to G. During settling, the value of $Q$ should remain constant unless Zr in solution reacts with Fe from the crucible walls or is oxidized. If this occurs, then $Q$ decreases due to a loss of soluble Zr taking the grain size from G to H. These reactions will be more likely if the melt is held at high temperature for long periods. Assuming no deleterious reactions occur and the melt is restirred after settling has occurred, the grain size will then decrease from G to D.

To test the predictions of Figure 6, experiments were carried out on a Mg-0.5 pct Zn alloy. The steps from A to B, D, E, F, and G were carried out as described in the caption for Figure 7. It was found that the grain size changes observed correspond very well with the predictions of the schematic representation given in Figure 6. The soluble Zr contents of the samples were analyzed and Figure 8 plots the measured grain size against $1/Q$ calculated from the analyzed Zr contents. Good agreement with the model illustrated in Figure 6 is obtained. Because of the variation in insoluble Zr content among the samples analyzed, it was not possible to calculate the value of $b$ for Zr particles. A more extensive set of experiments is required. To be able to reduce the cost of Zr addition, we need to quantify the relationships to obtain values for $b$ and $a$ and relate them


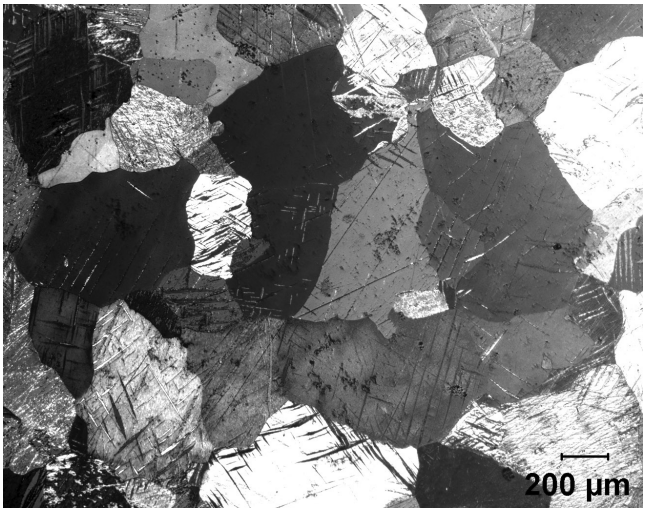

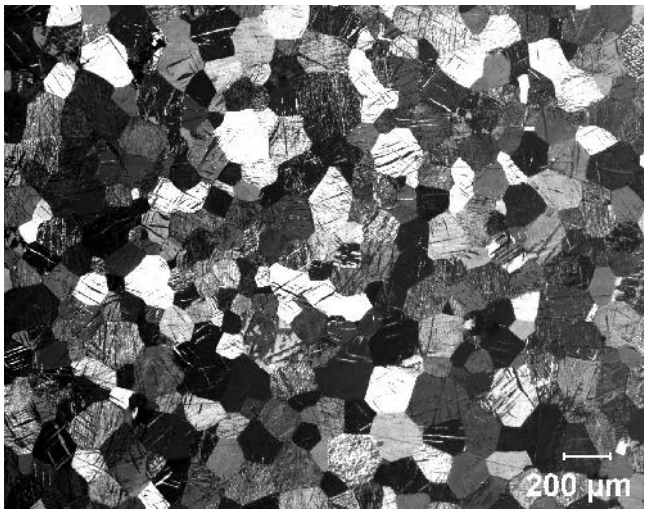


(*d*)

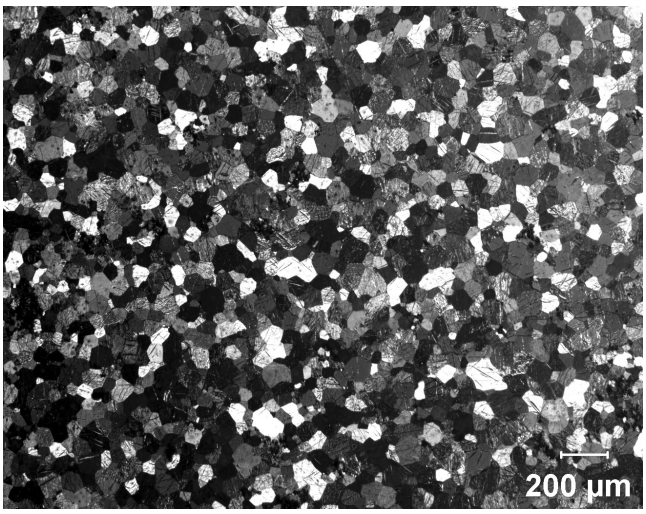


(*e*)

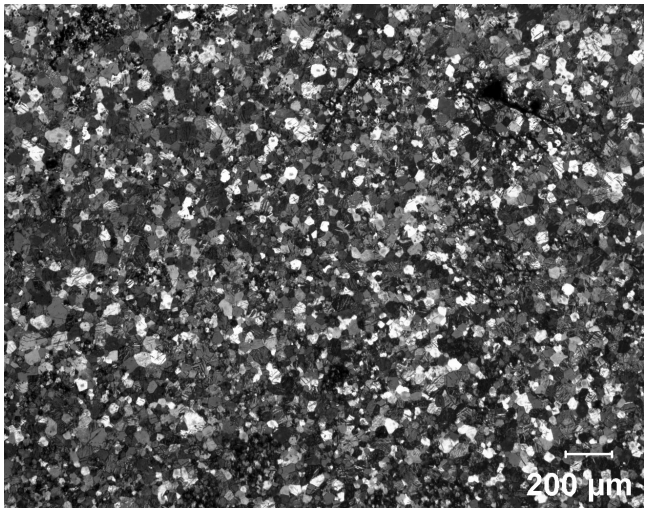


(*f*)

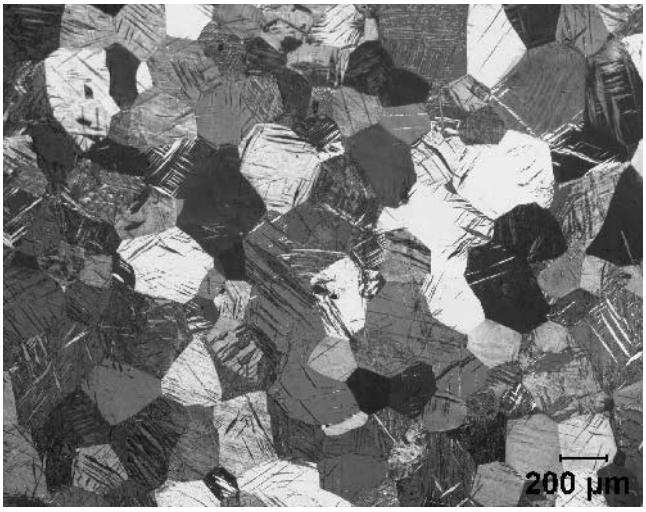


(*g*)

Fig. 7—(Continued). Experimental assessment of the model presented in Fig. 6 on a Mg-0.5 pct Zn alloy. The Micrograph code corresponds to the sample codes A, B etc. shown in Fig. 6. For example, Micrograph A corresponds to point A on Fig. 6 and has a grain size of 590 $\mu$m. Micrograph B with a grain size of 350 $\mu$m was obtained after 0.5 pct Zr was added to the melt in the absence of stirring. After 2 min of stirring, the grain size further decreased to 110 $\mu$m (micrograph D) due to dissolution of Zr (increasing $Q$) and a more even distribution of Zr particles. Micrograph E is the result of a further addition of 0.5 pct Zr (total 1 pct Zr) that increases $Q$ toward the solubility limit and adds extra Zr particles together reducing the grain size to 54 $\mu$m, and micrograph F results from another 1 pct Zr addition (total 2 pct Zr), which brings $Q$ close to the solubility limit and increases the number of Zr particles further reducing the grain size to 27 $\mu$m. Micrograph G shows the effect of holding the melt that produced D for 2 hours without stirring. The settling of Zr particles causes the grain size to reduce to 200 $\mu$m. When the melt is restirred for 2 minutes, the grain size returns to 110 $\mu$m. The alloys were melted in an aluminum titanite crucible and the sampling temperature was 730 °C.

to actual soluble and insoluble Zr contents. This information will allow calculation of the exact amount of Zr addition needed to deliver the required grain size and definition of the processing conditions to prevent wastage due to settling and reaction with the crucible walls and the atmosphere.

## V. SUMMARY

The literature on the grain refinement of magnesium alloys was reviewed according to two groups of magnesium alloys: aluminum-bearing and aluminum-free alloys. It is concluded that the understanding of grain refinement in aluminum-bearing alloys is not complete and more knowledge is required about the role of impurities and the addition of further alloying elements in affecting the potency of nucleant particles. A number of grain-refining methods have been developed but they suffer from a number of problems making them unsuitable for commercial casting operations. Also, the response to grain refinement by these methods due to purity and casting condition differences is not readily predictable. This lack of predictability and understanding may explain why a commercially suitable grain refiner for aluminum-bearing alloys has not been developed. In contrast, aluminum-free alloys are readily

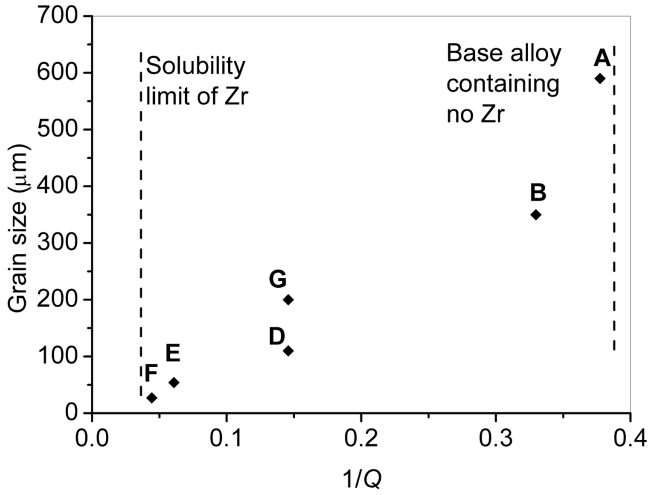


Fig. 8—The experimentally determined grain sizes plotted against 1/*Q* calculated from the measured soluble Zr contents for alloys A, B, D, E, F, and G. There is good agreement with the schematic representation in Fig. 6.

refined by Zr, and this method of refinement is well established scientifically and commercially. However, Zr additions are expensive and optimization of Zr refinement to reduce cost is necessary.

Therefore, research needs to focus on gaining a better understanding of the detailed mechanisms by which refinement occurs and gathering data to improve the ability to predict grain refinement for particular combinations of alloy and impurity chemistry and nucleant particles. A model that was developed for aluminum alloys was presented that takes into account both alloy chemistry and nucleant particle potency. This model was then applied to experimental data from a range of magnesium alloys. It was shown that by using this analytical approach, new information on the refinement of magnesium alloys is obtained as well as providing a method of characterizing the effectiveness of new refiners. The new information revealed by the model has identified new directions for further research.

## ACKNOWLEDGMENTS

The authors acknowledge the support of the Cooperative Research Centre for Cast Metals Manufacturing (CAST). CAST was established and is supported by the Australian Government's Cooperative Research Centres Program. Also acknowledged is the Australian Magnesium Corporation for their ongoing support for research into the grain refinement of magnesium alloys, the University of Queensland for sponsoring Peng Cao's postgraduate scholarship, and the Australian Research Council and Australian Magnesium Corporation for funding Zoë Hildebrand's scholarship.

## REFERENCES

1. C.J. Bettles, C.T. Forwood, D.H. StJohn, M.T. Frost, D.S. Jones, M. Qian, G.L. Song, J.R. Griffiths, and J.F. Nie: *Magnesium Technology 2003*, San Diego, CA, 2003, H.I. Kaplan, ed., TMS, Warrendale, PA, 2003, pp. 223-26.
2. G.L. Song and A. Atrens: *Adv. Eng. Mater*., 2003, vol. 5, pp. 837-58.
3. V. Kondic: *Metallurgical Principles of Founding*, Edward Arnold, London, 1968, pp. 100-03.
4. I.G. Farbenindustrie: British Patent GB359,425, 1931.
5. E.F. Emley: *Principles of Magnesium Technology*, Pergamon Press, Oxford, United Kingdom, 1966, pp. 206-23.
6. C.E. Nelson: *Trans. AFS*, 1948, vol. 56, pp. 1-23.
7. N. Tiner: *AIME Tech. Pub*., 1945, vol. 12 (7), pp. 1-19.
8. Y. Tamura, T. Haitani, E. Yano, T. Motegi, N. Kono, and E. Sato: *Mater. Mater. Trans. A*, 2002, vol. 33A, pp. 2784-88.
9. P. Cao, M. Qian, and D.H. StJohn: *Scripta Mater*., 2004, vol. 51, pp. 125-29.
10. J.Y. Byun, S. Kwon, H.P. Ha, and J.K. Yoon: *Magnesium Alloys and Their Applications*, K.U. Kainer, ed., Wiley-VCH, New York, NY, 2003, pp. 713-18.
11. K. Achenbach, H.A. Nipper, and E. Piwowarsky: *Die Giesserei*, 1939, vol. 26, pp. 597-604 and 621-623.
12. C.H. Mahoney, A.L. Tarr, and P.E. LeGrand: *Trans. AIME*, 1945, vol. 161, pp. 328-50.
13. J.A. Davis, L.W. Eastwood, and J. DeHaven: *Trans. AFS*, 1945, vol. 53, pp. 352-62.
14. M. Qian and P. Cao: *Scripta Mater*., 2005, vol. 52, pp. 415-19.
15. Y. Liu, X. Liu, and B. Xiufang: *Mater. Lett*., 2004, vol. 58, pp. 1282-87.
16. E. Yano, Y. Tamura, T. Motegi, and E. Sato: *J. Jpn. Inst. Light Met*., 2001, vol. 51 (11), pp. 594-98.
17. I.G. Farbenindustrie: Belgian Patent 444,757, 1942.
18. T. Motegi, E. Yano, Y. Tamura, and E. Sato: *Mater. Sci. Forum*, 2000, vols. 350–351, pp. 191-98.
19. S. Boily and M. Blouin: Canadian Patent 2,327,950, 2002.
20. N. Nishino, H. Kawahara, Y. Shimizu, and H. Iwahori: in *Magnesium Alloys and Their Applications*, K.U. Kainer, ed., Wiley-VCH, New York, NY, 2000, pp. 59-64.
21. Y.C. Lee, A.K. Dahle, and D.H. StJohn: *Metall. Mater. Trans. A*, 2000. vol. 31A, pp. 2895-2905.
22. E.F. Emley: *Principles of Magnesium Technology*, Pergamon Press, Oxford, United Kingdom, 1966, pp. 126-56.
23. H. Okamoto: *J. Phase Equilibria*, 2002, vol. 23 (2), pp. 198-99.
24. M. Qian, D.H. StJohn, and M.T. Frost: in *Magnesium Alloys and Their Applications*, K.U. Kainer, ed., Wiley-VCH, Wolfsburg, 2003, pp. 706-12.
25. S. Housh, B. Mikucki, and A. Stevenson: *Metals Handbook*, ASM INTERNATIONAL, Materials Park, OH, 1990, pp. 455-79.
26. B.R. Powell, L.J. Ouiment, J.E. Allison, J.A. Hines, R.S. Beals, L. Kopka, and P.P. Ried: *Magnesium Technology 2004*, Charlotte, NC, 2004, A.A. Luo, ed., TMS, Warrendale, PA, 2004, pp. 1-9.
27. M. Qian, D.H. StJohn, and M.T. Frost: *Scripta Mater*., 2002, vol. 46, pp. 649-54.
28. D.H. StJohn, A.K. Dahle, T. Abbott, M.D. Nave, and M. Qian: *Magnesium Technology 2003*, San Diego, CA, 2003, H.I. Kaplan, ed., TMS, Warrendale, PA, 2003, pp. 95-100.
29. P. Cao, M. Qian, D.H. StJohn, and M.T. Frost: *Mater. Sci. Technol*., 2004, vol. 20, pp. 585-92.
30. F. Sauerwald: *Z. Metallkd*., 1949, vol. 40, pp. 41-46.
31. Y. Tamura, N. Kono, T. Motegi, and E. Sato: *J. Jpn. Inst. Light Met*., 1998, vol. 48, pp. 185-89.
32. M. Qian, D.H. StJohn, and M.T. Frost: in *Magnesium Technology 2003*, San Diego, CA, 2003, H.I. Kaplan, ed., TMS, Warrendale, PA, 2003, pp. 215-20.
33. M. Qian, D.H. StJohn, and M.T. Frost: *Mater. Sci. Forum*, 2003, vols. 419–422, pp. 593-98.
34. M. Qian, D.H. StJohn, and M.T. Frost: in *Magnesium Technology 2003*, San Diego, CA, 2003, H.I. Kaplan, ed., TMS, Warrendale, PA, 2003, pp. 209-14.
35. M. Qian, L. Zheng, D. Graham, M.T. Frost, and D.H. StJohn: *J. Light Met*., 2001, vol. 1, pp. 157-65.
36. Z. Hildebrand, M. Qian, D.H. StJohn, and M.T. Frost: in *Magnesium Technology 2004*, A.A. Luo, ed., TMS, Warrendale, PA, 2004, pp. 241-45.
37. M. Qian, D.H. StJohn, and M.T. Frost: *Scripta Mater*., 2004, vol. 50, pp. 1115-19.
38. A. Cibula: *J. Inst. Met*., 1949, vol. 76, pp. 321-60.
39. F.A. Crossley and L.F. Mondolfo: *J. Met*., 1951, vol. 191, pp. 1143-51.
40. I. Maxwell and A. Hellawell: *Acta Mater*., 1975, vol. 12, pp. 229-37.
41. M.A. Easton and D.H. StJohn: *Metall. Mater. Trans. A*, 1999, vol. 30A, pp. 1613-23.

42. D.G. McCartney: *Int. Mater. Rev*., 1989. vol. 34 (5), pp. 247-60.
43. M. Johnsson: *Z. Metallkd*., 1994, vol. 85, pp. 781-85.
44. A.L. Greer, A.M. Bunn, A. Tronche, P.V. Evans, and D.J. Bristow: *Acta Mater*., 2000, vol. 48 (11), pp. 2823-35.
45. M.A. Easton and D.H. StJohn: *Acta Mater*., 2001, vol. 49, pp. 1867-78.
46. P. Desnian, Y. Fautrelle, J.-L. Meyer, J.P. Riquet, and F. Durand: *Acta Metall. Mater*., 1990, vol. 41, pp. 1513-23.
47. M.A. Easton and D.H. StJohn: *Alum. Trans*., 1999, vol. 1, pp. 51-58.
48. M.A. Easton and D.H. StJohn: *Metall. Mater. Trans. A,* in press.
49. A. Luo: *Can. Metall. Q*., 1996, vol. 35, pp. 375-83.
50. M. Qian, D. Graham, L. Zheng, D.H. StJohn, and M.T. Frost: *Mater. Sci. Technol*., 2003, vol. 19, pp. 156-62.
51. M.A. Easton and D.H. StJohn: *Metall. Mater. Trans. A*, 1999, vol. 30A, pp. 1625-33.